Notch Inhibits Expression of the Krüppel-Like Factor 4 Tumor Suppressor in the Intestinal Epithelium

Amr M. Ghaleb[1], **Gaurav Aggarwal**[1], **Agnieszka B. Bialkowska**[1], **Mandayam O. Nandan**[1], and **Vincent W. Yang**[1,2,*]

1 *Division of Digestive Diseases, Department of Medicine, Winship Cancer Institute, Emory University School of Medicine Atlanta, GA*

2 *Department of Hematology and Oncology, Winship Cancer Institute, Emory University School of Medicine Atlanta, GA*

Abstract

The zinc finger-containing transcription factor, Krüppel-like factor 4 (KLF4), inhibits cell proliferation. An *in vivo* tumor suppressive role for KLF4 is demonstrated by the recent finding that *Klf4* haploinsufficiency in $Apc^{Min/+}$ mice promotes intestinal tumorigenesis. Studies also show that KLF4 is required for the terminal differentiation of goblet cells in the mouse intestine. The Notch signaling pathway suppresses goblet cell formation and is up-regulated in intestinal tumors. Here we investigated the relationship between Notch signaling and KLF4 expression in intestinal epithelial cells. The rate of proliferation of HT29 human colon cancer cells was reduced when treated with the γ-secretase inhibitor dibenzazepine (DBZ) to inhibit Notch or siRNA directed against Notch. KLF4 levels were increased in DBZ- or Notch siRNA-treated cells. Conversely, over-expression of Notch in HT29 cells reduced KLF4 levels, suppressed *KLF4* promoter activity and increased proliferation rate. Treatment of $Apc^{Min/+}$ mice with DBZ resulted in a 50% reduction in the number of intestinal adenomas compared to the vehicle-treated group ($p < 0.001$). Both the normal-appearing intestinal mucosa and adenomas obtained from DBZ-treated $Apc^{Min/+}$ mice had increased goblet cell numbers and Klf4 staining accompanied by reduced cyclin D1 and Ki67 staining when compared to those from vehicle-treated mice. Results of these studies indicate that Notch signaling suppresses KLF4 expression in intestinal tumors and colorectal cancer cells. Inhibition of Notch signaling increases KLF4 expression and goblet cell differentiation, and reduces proliferation and tumor formation. KLF4 is therefore a potential mediator for the anti-tumor effect of Notch inhibitors such as DBZ.

Keywords

KLF4; goblet cells; γ-secretase inhibitor; $Apc^{Min/+}$ mouse; adenomas

INTRODUCTION

Krüppel-like factor 4 (KLF4) is a zinc finger-containing transcription that is highly expressed in the terminally differentiated epithelial cells of the intestine (1–3). Biochemical studies indicate that KLF4 inhibits cell proliferation by blocking progression of the cell cycle at the G_1/S and G_2/M transitions (4–7). Studies also show that expression of KLF4 is reduced in colorectal neoplasia including carcinoma and adenoma relative to normal mucosa (8–11).

*Corresponding Author: Vincent W. Yang, M.D., Ph.D., Division of Digestive Diseases, Department of Medicine, Winship Cancer Institute, Emory University School of Medicine, 201 Whitehead Research Building, 615 Michael Street, Atlanta, GA 30322; Tel: (404) 727-5638; Fax: (404) 727-5767; E-mail: vyang@emory.edu.

Finally, we recently reported that haploinsufficiency of *Klf4* promotes the development of intestinal adenomas in $Apc^{Min/+}$ mice (12). Taken together, these studies are highly suggestive that KLF4 functions as a tumor suppressor in the intestinal epithelium.

Notch genes encode large, single trans-membrane receptors that regulate a broad spectrum of cell fate decisions (13,14). Notch activity is dependent on ligand binding followed by a series of proteolytic cleavage and subsequent nuclear translocation of its cytoplasmic domain, Notch intracellular domain (NICD). NICD then complexes with the DNA-binding protein RBP-J (also known as CSL or CBF1) and Mastermind-like 1 (MAML1) to exert a transcriptional effect on target gene expression (13–17). The best characterized Notch target gene is the basic helix-loop-helix (bHLH) protein hairy/enhancer of split (HES) (18). One of the proteolytic enzymes involved in cleaving the membrane-bound Notch is a γ-secretase that includes the presenillin proteins, PS1 and PS2, which are often mutated in familial Alzheimer's disease (19). Inhibition of γ-secretase blocks activation of the Notch pathway (19,20).

The intestinal epithelium is composed of two distinct cell lineages, one absorptive and the other secretory in nature (21). Mutational studies of the Notch downstream target HES1 in mice have revealed that the Notch pathway is involved in cell fate decision in the intestinal epithelium (22). Thus, targeted deletion of *Hes1* results in a relative increase in secretory cells at the expense of absorptive cells in the fetal intestine (22). Similarly, conditional deletion of *Rbp-j* from the intestinal epithelium leads to the conversion of proliferative crypt cells into post-mitotic goblet cells (23). A recent study describing an increase in secretory cells relative to absorptive cells in the intestines of zebrafish that are mutant for a Notch ligand, *DeltaD*, also supports a role for Notch signaling in cell fate decision (24). Importantly, treatment of $Apc^{Min/+}$ mice, a model for intestinal tumorigenesis (25), with a γ-secretase inhibitor results in goblet cell differentiation in the adenomas derived from the intestine (23). Moreover, Notch signaling has been previously shown to be up-regulated in intestinal tumors (23,26). Taken together, these studies imply that Notch inhibition by γ-secretase inhibitors may have a therapeutic potential in the treatment of intestinal neoplasm.

Previous studies also implicate a role for KLF4 in cell fate decision in the intestinal epithelium. Newborn mice with homozygous deletion of *Klf4* have a 90% reduction in the number of goblet cells in their colon and lack normal goblet cell morphology by ultrastructural analysis (27). Similarly, mice with conditional deletion of *Klf4* from the cornea demonstrate a loss of conjunctival goblet cells (28). Because both KLF4 and Notch are involved in regulating cell proliferation and cell fate decision, we sought to investigate the relationship between Notch signaling and KLF4 expression in the current study.

MATERIALS AND METHODS

Cell lines, reagents and plasmid constructs

The human colon cancer cell line HT29 was obtained from the American Type Culture Collection (Manassas, VA) and maintained in Dulbecco's Modified Eagle's Medium (DMEM) supplemented with 10% fetal bovine serum (FBS). The γ-secretase inhibitor, dibenzazepine (DBZ), was purchased from Sigma-Aldrich (St. Louis, MO), and dissolved in dimethylsulfoxide (DMSO) (EMDchemicals, Gibbstown, NJ). For *in vitro* experiments, solubilized DBZ was suspended in growth medium containing 0.01% (v/v) Tween 80 to the final concentrations as indicated. Antibodies used for Western blot analyses were obtained from the following sources: rabbit anti-KLF4 (H180), rabbit anti-p57 (C20), and rabbit anti-p27 (Santa Cruz Biotechnology, Santa Cruz, CA); mouse monoclonal anti-full-length (FL) Notch (Abcam, Cambridge, MA); rabbit anti-NICD (Millipore, Billerica, MA); mouse monoclonal anti-p21 (BD Biosciences, San Jose, CA); mouse monoclonal anti-β-actin (BD

Biosciences); rabbit anti-cleaved caspase-3 and rabbit anti-cleaved poly (ADP-ribose) polymerase (PARP) (Cell Signaling Tech., Danvers, MA).

The expression construct containing full-length (FL)-Notch1 (pCS2-MT-Notch1) (29) was kindly provided by Dr. Raphael Kopan of Washington University, St. Louis, MO, and those containing NICD (MIGR1-ICNX) (30) and dominant-negative MAML1 peptide [MIGR1-MAML1(13–74)] (31) were kindly provided by Dr. Warren Pear of University of Pennsylvania, Philadelphia, PA. The expression vector expressing human HES1 (pCMV-HES1) was purchased from Origene (Rockville, MD). A construct linking 1.0 kb of the 5′-flanking region and 550 bp of the untranslated region of the mouse *Klf4* gene to the pGL2-basic luciferase reporter (Promega; Madison, WI), pGL2-Klf4, was previously generated in our laboratory (32). Small interfering (siRNA) directed against human Notch was obtained from Invitrogen (Carlsbad, CA).

Treatment of animals with the γ-secretase inhibitor DBZ and assessment of tumor burden

Apc^{Min/+} mice on a B6 background were crossbred. Wild type B6 mice served as controls. DBZ solubilized in DMSO was suspended in phosphate-buffered saline (PBS) containing 0.5% (w/v) hydroxypropylmethylcellulose (Methocel E4M) (Dow chemicals, Midland, MI) and 0.01% (v/v) Tween 80, as vehicle (23), to the final concentrations indicated below. At 10, 14 and 18 weeks, mice were given intraperitoneal injections of 10 μmol/kg DBZ or carrier alone every other day for a total of 10 days. Two days following the last injection (on weeks 12, 16 and 20), mice were euthanized by CO_2 asphyxiation and the small and large intestine longitudinally dissected in their entirety. After washing in PBS, the intestines were examined under a dissection microscope for the presence of adenomas. The number and size of adenomas in both the small and large intestine were recorded. Adenomas identified in the small and large intestine were grouped by size (<1 mm, 1–2 mm, 2–3 mm, and >3 mm).

Alcian blue/periodic acid Schiff (AB/PAS) staining for goblet cells

Goblet cell staining was carried out as described (see footnote)[1] with slight modifications. In brief, intestinal tissues were fixed in 10% formalin in PBS and subsequently embedded in paraffin. Five μm-thick paraffin sections were cut and applied to Superfrost Plus slides (VWR, West Chester, PA). Sections were deparaffinized in xylene, rehydrated in ethanol then brought to distilled water for 5 min. Alcian blue (1% (w/v) Alcian blue 8GX (Sigma-Aldrich) in 3% acetic acid) was applied to the sections for 15 min at RT, followed by 2 min wash in running tap water. Periodic acid (Biocare Medical, Concord, CA) was then applied for 5 min at RT, slides washed in distilled water, and then stained with Schiff's reagent (Biocare Medical) for 15 min at RT, followed by 5 min wash in running tap water. The sections were then counterstained for nuclei with Nuclear Fast Red (Biocare Medical) for 15 min then washed in running tap water for 2 min, followed by dehydration (twice in 95% EtOH then twice in 100% EtOH) and cover-slipping.

Immunohistochemistry (IHC)

Intestinal tissues for IHC were fixed in 10% formalin in PBS and subsequently embedded in paraffin. Five μm-thick paraffin sections were cut and applied to Superfrost Plus slides. Sections were deparaffinized in xylene, rehydrated in ethanol, and then treated with 10 mM Na citrate buffer, pH 6.0, at 120 °C for 10 min in a pressure cooker. The histological sections were incubated with a blocking buffer (2% non-fat dry milk, 0.01% Tween 20, in PBS) for 1 hr at room temperature. An avidin/biotin blocking kit (Vector Laboratories, Burlingame, CA) was used in conjunction with the blocking buffer according to manufacturer's directions to

---

[1]Footnote: http://www.ihcworld.com/protocols/special_stains/alcian_blue_pas_ellis.htm

reduce background and nonspecific secondary antibody binding. Sections were then stained for Klf4 (rabbit anti-GKLF (H-180); Santa Cruz Biotechnology), Cyclin D1 (rabbit mono-clonal anti-cyclin D1; Biocare Medical), and Ki67 (rabbit anti-Ki67; Abcam, Cambridge, MA) at a dilution of 1:200, 1:100, and 1:1,000, respectively, in the blocking buffer overnight at 4° C. Detection of primary antibodies was carried out using appropriate biotinylated secondary antibodies at 1:500 dilutions for 20 min at RT, and color development was performed using the Vectastain ABC kit (Vector Laboratories). Sections were then counterstained with hematoxylin, dehydrated, and cover-slipped. Sections were also stained separately for goblet cells using Alcian blue/periodic acid stain. Images were acquired using an Axioskop 2 plus microscope (Zeiss, Thornwood, NY) equipped with an AxioCam MRC5 CCD camera (Zeiss).

Trypan Blue stain for viable cell count

Following trypsinization, cells were collected by low speed centrifugation, washed once in PBS and resuspended in 200 μl PBS. An equal volume of 0.4% Trypan Blue stain (Mediatech, Inc, Herndon, VA) was added to the cell suspension, mixed gently, allowed to stand for 5 min at RT and then percent of viable (unstained) and dead (stained) were counted using a hemocytometer.

Flow cytometry

Cell cycle analysis by fluorescence-activated cell sorter (FACS) was performed as previously described (5). Cells were rinsed twice in PBS, treated with trypsin and resuspended in their corresponding medium containing 10% FBS. Cells were then collected by centrifugation, washed with PBS, collected again by centrifugation, resuspended in 70% ethanol and fixed at −20°C overnight. Cells were pelleted once again by centrifugation and resuspended in a solution containing 50 mg/ml propidium iodide, 50 mg/ml RNase A, 0.1% Triton X-100 and 0.1mM ethylene diamine tetra acetic acid (EDTA) at room temperature for 30min. Flow cytometry was performed on a FACSCalibur cytometer (Becton Dickinson, Franklin Lakes, NJ, USA).

RESULTS

Suppression of Notch signaling in HT29 cells by DBZ reduces proliferation and increases KLF4 levels

We first determined the effect of Notch inhibition on the rate of proliferation and KLF4 expression in the HT29 human colon cancer cells. HT29 cells were treated for progressively longer periods of time with increasing amounts of the γ-secretase inhibitor, DBZ, to inhibit Notch signaling. As seen in Figure 1A, there was a gradual reduction in the rate of proliferation of HT29 cells with increasing concentrations of DBZ when compared to control. To determine whether the decreased rate of proliferation was due to cell death from drug toxicity, we measured viable cell counts using Trypan Blue staining and FACS analysis as well as Western blotting for cleaved caspase-3 and cleaved PARP. As seen in Supplementary Figure 1A, there were no significant differences in cell viability between treated and untreated cells at all time points as measured by Trypan Blue exclusion. There were also no significant differences in the percentages of cells in the sub-G_1 population between treated and untreated cells as measured by flow cytometry (Supplementary Figure 1B). Moreover, there were no detectable levels of either cleaved caspase-3 or cleaved PARP at any given drug concentration and time point (Supplementary Figure 1C). These results indicate that the effect of DBZ on HT29 cells is mainly due to inhibition of cell proliferation rather than induction of apoptosis.

Western blot analysis of proteins extracted from HT29 cells treated with various concentrations of DBZ for various periods of time showed a dose-dependent reduction in the levels of the activated form of Notch, NICD, along with a dose-dependent increase in the levels of KLF4

(Figure 1B). The increase in KLF4 levels was accompanied by an increase in the levels of p21 (Figure 1B), a downstream mediator of KLF4's cell cycle effect (4). In contrast, there was only a modest increase in the levels of p27 but no change in the levels of p57 upon treatment of DBZ (Supplementary Figure 2).

Notch signaling inhibits expression of KLF4 in HT29 cells

To independently confirm the observation that suppression of Notch signaling with DBZ results in the increase in KLF4, we inhibited Notch using siRNA and determined the effect of such suppression on KLF4 expression. As with DBZ, suppression of Notch by siRNA targeted against full-length Notch resulted in elevated levels of KLF4 mRNA and protein (Figures 2A and 2B, respectively). Conversely, the level of KLF4 was reduced upon over-expression of either NICD or full-length Notch in HT29 cells (Figure 2C).

We then correlated Notch activity with the rate of cell proliferation following genetic manipulations in HT29 cells. As seen in Supplementary Figure 3A, over-expression of NICD increased the rate of proliferation of HT29 cells. Conversely, inhibition of Notch by siRNA reduced the rate of proliferation (Supplementary Figure 3B), in a manner that is similar to inhibition of Notch by DBZ (Figure 1A). These experiments further demonstrate that Notch promotes proliferation of HT29 cells and inhibits KLF4 expression.

In addition to inhibiting KLF4 expression at the levels of mRNA and protein as shown in Figures 2A to 2C, activation of Notch by over-expression of NICD in HT29 cells led to a decrease in the luciferase activity directed by the mouse *Klf4* promoter (Figure 2D; compare lanes 1 and 2). Moreover, co-transfection of the dominant-negative MAML1 (dn-MAML1) abrogated the ability of NICD to suppress *Klf4* promoter activity in a dose-dependent manner (Figure 2D; lanes 4–7). These results indicate that Notch inhibits KLF4 expression by suppressing *KLF4* promoter.

HES1, a transcription repressor, is a known to mediate Notch signaling. Sequence analysis of 1.0 kb of the 5′-flanking sequence and 550 bp of the 5′-untranslated region of the mouse *Klf4* gene (32) revealed five potential HES1 binding sites (18,33) (Supplementary Figure 4). Consequently, co-transfection experiments showed that HES1 significantly reduced luciferase activity driven by the *Klf4* promoter (Figure 2E; compare lanes 1 and 2). Of note is that over-expression of dn-MAML1 had no effect on the ability of HES1 to suppress *Klf4* promoter activity (Figure 2E; lanes 4–7). This is consistent with previous findings that MAML1 exerts its effect on NICD but not HES1 (13–18). Deletion analysis of the *Klf4* promoter showed that the minimal region required for HES1 to suppress *Klf4* promoter activity is between nt −168 and +144 (32), a region that contains a single reverse class C HES1-binding sequence (Supplementary Figure 4 and data not shown). These results demonstrate that HES1 is the mediator for the suppressive effect of Notch on the KLF4 promoter.

DBZ treatment results in a reduction of the number of intestinal adenomas in *Apc^Min/+* mice

To determine whether inhibition of Notch signaling has an effect on intestinal tumor formation *in vivo*, we treated *Apc^Min/+* mice at ages 10, 14 and 18 weeks with 10 μmol/kg DBZ or vehicle alone every other day for a total of 10 days. The number of adenomas in the intestine was assessed 2 days following the last injection. As seen in Figure 3A, there was on average a 50% reduction in the number of adenomas in the small intestine of DBZ-treated *Apc^Min/+* mice compared to vehicle-treated *Apc^Min/+* mice ($p < 0.001$ by paired two-tailed *t*-test) combining all three age groups. There was no statistical difference in the number of adenomas in the colons of DBZ- and vehicle-treated *Apc^Min/+* mice although the average number of colonic adenomas per mouse was fewer than two (data not shown). When the tumor burdens at the three different ages were separately analyzed (Figure 3B), there was a statistically significantly reduction in

the number of small intestinal adenomas per mouse at weeks 12 and 16 ($p < 0.005$ and < 0.01, respectively) in DBZ-treated mice when compared to control. At 20 weeks, there was a trend towards reduction in the number of small intestinal adenomas due to DBZ treatment although the difference did not reach statistical significance ($p = 0.07$).

We also examined whether there were any differences between the size of adenomas formed in the small and large intestines of DBZ-treated $Apc^{Min/+}$ mice and control. As shown in Figure 3C, the adenomas developed in the small intestines of $Apc^{Min/+}$ mice at 12 weeks were mostly small (<1 mm and 1–2 mm). By week 16, there was a shift in the size of adenomas to larger ones and this trend continued at 20 weeks. DBZ-treated $Apc^{Min/+}$ mice had a similar pattern of size distribution of adenomas as the vehicle-treated $Apc^{Min/+}$ mice at any given age although there was a significant reduction in the number of adenomas in some of the size range per age group in the treated $Apc^{Min/+}$ mice as compared to control mice (indicated by double headed arrows). There was no significant difference in the size of adenomas formed in the large intestines of untreated and treated $Apc^{Min/+}$ mice (data not shown).

DBZ treatment leads to increased numbers of goblet cells and Klf4 levels in the intestinal mucosa of wild type and $Apc^{Min/+}$ mice

Previous studies indicate that DBZ treatment in mice leads to intestinal goblet cell metaplasia (23,34). To confirm these findings and to investigate whether DBZ treatment results in increased Klf4 expression *in vivo*, we examined intestinal tissues obtained from DBZ- or vehicle-treated wild type and $Apc^{Min/+}$ mice using alcian blue/periodic acid-Schiff (AB/PAS) staining to identify goblet cells and immunostaining to identify Klf4. Results in Figure 4 show that both the number of goblet cells and the intensity of Klf4 immunostain (panels C and D, respectively) were increased in the normal-appearing small intestinal mucosa from $Apc^{Min/+}$ mice treated with DBZ when compared to vehicle-treated mice (panels A and B). A similar increase in both is noted in the wild type mice treated with DBZ (Supplementary Figure 5). Importantly, the number of goblet cells and Klf4 staining (Figure 5, panels C and D, respectively) were also increased in adenomas derived from the small intestines of DBZ-treated $Apc^{Min/+}$ mice as compared to control (Figure 5, panels A and B). In agreement with a previous report (23), the efficiency of the DBZ treatment in converting tumor cells into non-proliferating goblet cells was relatively low. In the large intestine, DBZ treatment led to only a modest increase in goblet cells and Klf4 staining in both wild type and $Apc^{Min/+}$ mice when compared to control mice (Supplementary Figures 6 and 7). This may explain the finding that DBZ treatment did not lead to a significant reduction in the number of large intestinal adenomas in $Apc^{Min/+}$ mice.

KLF4 has been shown to negatively regulate cell cycle progression (4,35). In addition to activating p21 expression (36), KLF4 is known to repress cyclin D1 expression (37). To determine whether DBZ-induced elevation in Klf4 expression in both normal intestinal mucosa and adenomas of $Apc^{Min/+}$ mice is correlated with changes in cyclin D1 levels and cellular proliferation, we performed immunostaining of intestinal tissues from DBZ- or vehicle-treated $Apc^{Min/+}$ mice for cyclin D1 and Ki67. As seen in Figure 6, cyclin D1 staining was significantly reduced in the crypts of the normal-appearing small intestinal mucosa in DBZ-treated $Apc^{Min/+}$ mice (panel C) compared to control (panel A). Similarly, cyclin D1 staining was reduced in intestinal adenomas obtained from DBZ-treated $Apc^{Min/+}$ mice (panel D) compared to control (panel B). A similar effect was observed for the Ki67 staining (Supplementary Figure 8). The reduced cyclin D1 and Ki67 may therefore explain the suppressive effect of DBZ on adenoma formation in $Apc^{Min/+}$ mice.

DISCUSSION

Previous studies indicate that KLF4 inhibits cell proliferation by activating crucial checkpoints in the cell cycle upon over-expression of exogenous KLF4 or following DNA damage (4–7, 35,38). A critical transcriptional target of KLF4 in these conditions is the cyclin-dependent inhibitor, p21 (4–7,35). These findings led to the suggestion that KLF4 may function as a tumor suppressor in colorectal cancer (8–11). Our recent study showing that haploinsufficiency of *Klf4* promotes the development of intestinal adenomas in *Apc^{Min/+}* mice supports this notion (12). *In vivo*, KLF4 has been shown to be required for the terminal differentiation of goblet cells in the colon (27) and conjunctiva (28) of newborn mice. Like KLF4, Notch pathways are known to be involved in cell fate decision (13,14). In the intestinal epithelium, Notch is active in the proliferative crypt compartment (22,39,40), in contrast to the preferential expression of KLF4 in the post-mitotic differentiated cell population (1,2). Deletion of key component of the Notch pathways such as Rbp-j and Hes1 from the intestine results in a shift from absorptive cells to secretory cells, including goblet cells (22,23). The opposing effects of KLF4 and Notch on cellular proliferation and goblet cell formation provide the rationale for our current study that attempts to establish a regulatory relationship between the two molecules.

Several lines of evidence from our studies indicate that KLF4 is a downstream target of Notch signaling. In HT29 cells, over-expression of either NICD or full-length Notch inhibits KLF4 expression and promoter activity (Figures 2C and 2D), which is accompanied by an increase in the rate of proliferation (Supplementary Figure 3A). Conversely, inhibition of Notch signaling by the γ-secretase inhibitor DBZ or siRNA against Notch results in an increase in KLF4 expression (Figures 1B, 2A and 2B) and a decrease in cellular proliferation (Figure 1A and Supplementary Figure 3B). In the normal intestinal mucosa of wild type or *Apc^{Min/+}* mice, DBZ treatment leads to an increase in Klf4 staining (Figure 4 and Supplementary Figure 5), which is accompanied by an increase in goblet cell numbers (Figure 4 and Supplementary Figure 5). A similar finding is noted in intestinal adenomas derived from *Apc^{Min/+}* mice (Figure 5). These findings strongly suggest that KLF4 is negatively regulated by Notch signaling. Upon inhibition of Notch, KLF4 expression is increased with an associated conversion of proliferative cells to goblet cells. Importantly, the increase in KLF4 is correlated with the anti-tumor activity of DBZ in *Apc^{Min/+}* mice (Figure 3) and the anti-proliferative effect of DBZ on the normal mucosa and adenomas from *Apc^{Min/+}* mice (Figure 6 and Supplementary Figure 8) and on HT29 cells (Figure 1A). In view of the established inhibitory effect of KLF4 on cell proliferation (1, 4, 7, 35), it is likely that KLF4 is responsible at least in part for the anti-tumor activity of DBZ.

Results of our studies indicate that Notch signaling negatively regulates the activity of the mouse *Klf4* promoter including 1.0 kb of the 5′-flanking region and 550 bp of the 5′-untranslated region (Figure 2D). Transcriptional regulation by Notch is dependent on the nuclear translocation and binding of NICD to the DNA binding protein RBP-J (also known as CSL or CBF1) and Mastermind-like1 (MAML1) (13–17), where MAML1 is required to stabilize the interaction between NICD and RBP-J (13, 14). HES1 is one of the best studied downstream targets and mediator of Notch signaling (18). Within the mouse *Klf4* promoter examined in this study, there are five potential binding sites for HES1 (Supplementary Figure 4). Indeed, co-transfection experiments show that both NICD and HES1 suppress *Klf4* promoter activity (Figures 2D and 2E). These experiments also show that a dominant-negative MAML1 construct is capable of competing with Notch but not HES1 in their ability to inhibit the *Klf4* promoter (Figures 2D and 2E). This is consistent with the fact that MAML1 regulates Notch signaling at the level of NICD and RBP-J but not at the level of HES1 (13–18).

Previous studies show that KLF4 level is reduced in intestinal adenomas from *Apc^{Min/+}* mice (12,41,42) and colonic adenomas from patients with familial adenomatous polyposis (42) when

compared to their respectively matched normal-appearing mucosa. Studies also indicate that KLF4 level is reduced in colorectal adenomas and carcinomas, and many colon cancer cell lines (8–11). Moreover, haploinsufficiency of *Klf4* results in an increase in intestinal tumor burden in *Apc*$^{Min/+}$ mice (12). Furthermore, KLF4 has been shown to regulate normal intestinal homeostasis and tumor repression by interacting with β-catenin and repressing β-catenin-mediated gene expression (43). Taken together, these studies corroborate the tumor suppressive effect of KLF4 in the intestinal epithelium. Importantly, ectopic expression of KLF4 in colorectal cancer cells that lack endogenous KLF4 expression results in reduced tumorigenecity (44). Results of the current study showing a correlation between Klf4 induction and cyclin D1 repression in the intestinal mucosa and adenomas of *Apc*$^{Min/+}$ mice as a consequence of DBZ treatment further highlight the significance of KLF4 in intestinal tumor development. The reduced cyclin D1 levels could be due to direct suppression of KLF4 on the cyclin D1 promoter (37) or indirect suppression of cyclin D1 expression as a consequence of the inhibitory effect of KLF4 on β-catenin (43). Be that as it may, the collective studies suggest that KLF4 is a potential therapeutic target for anti-tumor drugs.

A recent study shows that conditional ablation of Notch1 and Nothc2 or Rbp-j from the intestine of transgenic mice results in the derepression of p27 and p57 but not p21 (45). In comparison, our study shows that DBZ-mediated Notch inhibition in HT29 cells results in a significant induction in p21 (Figure 1B) but only a modest effect on p27 and no effect on p57 (Supplementary Figure 2). The differences seen between the two studies may be due to the difference in species (mouse vs. human) or methods of manipulation (genetic vs. pharmacological). It should be noted that KLF4 has recently been shown to activate expression of p27 in human pancreatic cells (46), suggesting that both p21 and p27 may play a role in the anti-proliferative effect of Notch inhibition.

Notch activity has been shown to be required for the maintenance of the proliferative progenitor crypt cells in the intestine (40). Overactivity of Notch in the intestine inhibits differentiation of the secretory lineage, including goblet cells (40). Conversely, suppression of Notch pathways by genetic (22,23) or pharmacological (23,34,47) means leads to goblet cell metaplasia. In view of the findings that KLF4 is required for terminal differentiation of goblet cells in the intestine (27) and that KLF4 induction is accompanied by increased goblet cell formation following DBZ treatment (this study), it is possible that KLF4 is the mediator for the goblet cell metaplasia secondary to treatment with γ-secretase inhibitors. Although goblet cell metaplasia following Notch suppression has been considered an undesirable toxic side effect (34,47,48), there is conceivably a therapeutic window between the anti-tumor and goblet cell metaplastic effect upon KLF4 induction. The exact mechanism by which up-regulation of KLF4 in the intestine after γ-secretase treatment leads to goblet cell metaplasia and reduction in adenoma formation is under investigation.

In conclusion, we demonstrate for the first time that the Notch cascade directly regulates KLF4 expression and that increased *Klf4* expression *in vivo* plays a role in the reduction of intestinal adenoma formation in *Apc*$^{Min/+}$ mice following Notch inhibition. Our findings suggest that events which inactivate KLF4 may promote tumorigenesis in human colorectal cancers, and that the reversal of the KLF4 inactivation, might lead to a reduction in the proliferation rate and ultimately a reduction in tumor burden.

Supplementary Material

Refer to Web version on PubMed Central for supplementary material.

Acknowledgements

References

1. Shields JM, Christy RJ, Yang VW. Identification and characterization of a gene encoding a gut-enriched Kruppel-like factor expressed during growth arrest. J Biol Chem 1996;271:20009–17. [PubMed: 8702718]

2. McConnell BB, Ghaleb AM, Nandan MO, Yang VW. The diverse functions of Kruppel-like factors 4 and 5 in epithelial biology and pathobiology. Bioessays 2007;29:549–57. [PubMed: 17508399]

3. Dang DT, Pevsner J, Yang VW. The biology of the mammalian Kruppel-like family of transcription factors. Int J Biochem Cell Biol 2000;32:1103–21. [PubMed: 11137451]

4. Chen X, Johns DC, Geiman DE, et al. Kruppel-like factor 4 (gut-enriched Kruppel-like factor) inhibits cell proliferation by blocking G1/S progression of the cell cycle. J Biol Chem 2001;276:30423–8. [PubMed: 11390382]

5. Yoon HS, Chen X, Yang VW. Kruppel-like factor 4 mediates p53-dependent G1/S cell cycle arrest in response to DNA damage. J Biol Chem 2003;278:2101–5. [PubMed: 12427745]

6. Yoon HS, Yang VW. Requirement of Kruppel-like factor 4 in preventing entry into mitosis following DNA damage. J Biol Chem 2004;279:5035–41. [PubMed: 14627709]

7. Ghaleb AM, Nandan MO, Chanchevalap S, et al. Kruppel-like factors 4 and 5: the yin and yang regulators of cellular proliferation. Cell Res 2005;15:92–6. [PubMed: 15740636]

8. Zhao W, Hisamuddin IM, Nandan MO, et al. Identification of Kruppel-like factor 4 as a potential tumor suppressor gene in colorectal cancer. Oncogene 2004;23:395–402. [PubMed: 14724568]

9. Wei D, Kanai M, Huang S, Xie K. Emerging role of KLF4 in human gastrointestinal cancer. Carcinogenesis 2006;27:23–31. [PubMed: 16219632]

10. Choi BJ, Cho YG, Song JW, et al. Altered expression of the KLF4 in colorectal cancers. Pathol Res Pract 2006;202:585–9. [PubMed: 16814484]

11. Xu J, Lu B, Xu F, et al. Dynamic down-regulation of Kruppel-like factor 4 in colorectal adenoma-carcinoma sequence. J Cancer Res Clin Oncol. 2008

12. Ghaleb AM, McConnell BB, Nandan MO, et al. Haploinsufficiency of Kruppel-like factor 4 promotes adenomatous polyposis coli dependent intestinal tumorigenesis. Cancer Res 2007;67:7147–54. [PubMed: 17671182]

13. Artavanis-Tsakonas S, Rand MD, Lake RJ. Notch signaling: cell fate control and signal integration in development. Science 1999;284:770–6. [PubMed: 10221902]

14. Baron M. An overview of the Notch signalling pathway. Semin Cell Dev Biol 2003;14:113–9. [PubMed: 12651094]

15. Liu ZJ, Xiao M, Balint K, et al. Inhibition of endothelial cell proliferation by Notch1 signaling is mediated by repressing MAPK and PI3K/Akt pathways and requires MAML1. Faseb J 2006;20:1009–11. [PubMed: 16571776]

16. Wallberg AE, Pedersen K, Lendahl U, Roeder RG. p300 and PCAF act cooperatively to mediate transcriptional activation from chromatin templates by notch intracellular domains in vitro. Mol Cell Biol 2002;22:7812–9. [PubMed: 12391150]

17. Wu L, Aster JC, Blacklow SC, et al. MAML1, a human homologue of Drosophila mastermind, is a transcriptional co-activator for NOTCH receptors. Nat Genet 2000;26:484–9. [PubMed: 11101851]

18. Iso T, Kedes L, Hamamori Y. HES and HERP families: multiple effectors of the Notch signaling pathway. J Cell Physiol 2003;194:237–55. [PubMed: 12548545]

19. Kopan R, Goate A. A common enzyme connects notch signaling and Alzheimer's disease. Genes Dev 2000;14:2799–806. [PubMed: 11090127]

20. De Strooper B, Annaert W, Cupers P, et al. A presenilin-1-dependent gamma-secretase-like protease mediates release of Notch intracellular domain. Nature 1999;398:518–22. [PubMed: 10206645]

21. van Es JH, Clevers H. Notch and Wnt inhibitors as potential new drugs for intestinal neoplastic disease. Trends Mol Med 2005;11:496–502. [PubMed: 16214417]

22. Jensen J, Pedersen EE, Galante P, et al. Control of endodermal endocrine development by Hes-1. Nat Genet 2000;24:36–44. [PubMed: 10615124]

23. van Es JH, van Gijn ME, Riccio O, et al. Notch/gamma-secretase inhibition turns proliferative cells in intestinal crypts and adenomas into goblet cells. Nature 2005;435:959–63. [PubMed: 15959515]

24. Crosnier C, Vargesson N, Gschmeissner S, et al. Delta-Notch signalling controls commitment to a secretory fate in the zebrafish intestine. Development 2005;132:1093–104. [PubMed: 15689380]

25. Moser AR, Pitot HC, Dove WF. A dominant mutation that predisposes to multiple intestinal neoplasia in the mouse. Science 1990;247:322–4. [PubMed: 2296722]

26. Veenendaal LM, Kranenburg O, Smakman N, et al. Differential Notch and TGFbeta signaling in primary colorectal tumors and their corresponding metastases. Cell Oncol 2008;30:1–11. [PubMed: 18219106]

27. Katz JP, Perreault N, Goldstein BG, et al. The zinc-finger transcription factor Klf4 is required for terminal differentiation of goblet cells in the colon. Development 2002;129:2619–28. [PubMed: 12015290]

28. Swamynathan SK, Katz JP, Kaestner KH, et al. Conditional deletion of the mouse Klf4 gene results in corneal epithelial fragility, stromal edema, and loss of conjunctival goblet cells. Mol Cell Biol 2007;27:182–94. [PubMed: 17060454]

29. Mumm JS, Schroeter EH, Saxena MT, et al. A ligand-induced extracellular cleavage regulates gamma-secretase-like proteolytic activation of Notch1. Mol Cell 2000;5:197–206. [PubMed: 10882062]

30. Pui JC, Allman D, Xu L, et al. Notch1 expression in early lymphopoiesis influences B versus T lineage determination. Immunity 1999;11:299–308. [PubMed: 10514008]

31. Weng AP, Nam Y, Wolfe MS, et al. Growth suppression of pre-T acute lymphoblastic leukemia cells by inhibition of notch signaling. Mol Cell Biol 2003;23:655–64. [PubMed: 12509463]

32. Mahatan CS, Kaestner KH, Geiman DE, Yang VW. Characterization of the structure and regulation of the murine gene encoding gut-enriched Kruppel-like factor (Kruppel-like factor 4). Nucleic Acids Res 1999;27:4562–9. [PubMed: 10556311]

33. Murata K, Hattori M, Hirai N, et al. Hes1 directly controls cell proliferation through the transcriptional repression of p27Kip1. Mol Cell Biol 2005;25:4262–71. [PubMed: 15870295]

34. Milano J, McKay J, Dagenais C, et al. Modulation of notch processing by gamma-secretase inhibitors causes intestinal goblet cell metaplasia and induction of genes known to specify gut secretory lineage differentiation. Toxicol Sci 2004;82:341–58. [PubMed: 15319485]

35. Chen X, Whitney EM, Gao SY, Yang VW. Transcriptional profiling of Kruppel-like factor 4 reveals a function in cell cycle regulation and epithelial differentiation. J Mol Biol 2003;326:665–77. [PubMed: 12581631]

36. Zhang W, Geiman DE, Shields JM, et al. The gut-enriched Kruppel-like factor (Kruppel-like factor 4) mediates the transactivating effect of p53 on the p21WAF1/Cip1 promoter. J Biol Chem 2000;275:18391–8. [PubMed: 10749849]

37. Shie JL, Chen ZY, Fu M, Pestell RG, Tseng CC. Gut-enriched Kruppel-like factor represses cyclin D1 promoter activity through Sp1 motif. Nucleic Acids Res 2000;28:2969–76. [PubMed: 10908361]

38. Whitney EM, Ghaleb AM, Chen X, Yang VW. Transcriptional profiling of the cell cycle checkpoint gene kruppel-like factor 4 reveals a global inhibitory function in macromolecular biosynthesis. Gene Expr 2006;13:85–96. [PubMed: 17017123]

39. Schroder N, Gossler A. Expression of Notch pathway components in fetal and adult mouse small intestine. Gene Expr Patterns 2002;2:247–50. [PubMed: 12617809]

40. Fre S, Huyghe M, Mourikis P, et al. Notch signals control the fate of immature progenitor cells in the intestine. Nature 2005;435:964–8. [PubMed: 15959516]

41. Ton-That H, Kaestner KH, Shields JM, Mahatanankoon CS, Yang VW. Expression of the gut-enriched Kruppel-like factor gene during development and intestinal tumorigenesis. FEBS Lett 1997;419:239–43. [PubMed: 9428642]

42. Dang DT, Bachman KE, Mahatan CS, et al. Decreased expression of the gut-enriched Kruppel-like factor gene in intestinal adenomas of multiple intestinal neoplasia mice and in colonic adenomas of familial adenomatous polyposis patients. FEBS Lett 2000;476:203–7. [PubMed: 10913614]

43. Zhang W, Chen X, Kato Y, et al. Novel cross talk of Kruppel-like factor 4 and beta-catenin regulates normal intestinal homeostasis and tumor repression. Mol Cell Biol 2006;26:2055–64. [PubMed: 16507986]

44. Dang DT, Chen X, Feng J, et al. Overexpression of Kruppel-like factor 4 in the human colon cancer cell line RKO leads to reduced tumorigenecity. Oncogene 2003;22:3424–30. [PubMed: 12776194]

45. Riccio O, van Gijn ME, Bezdek AC, et al. Loss of intestinal crypt progenitor cells owing to inactivation of both Notch1 and Notch2 is accompanied by derepression of CDK inhibitors p27Kip1 and p57Kip2. EMBO Rep 2008;9:377–83. [PubMed: 18274550]

46. Wei D, Kanai M, Jia Z, Le X, Xie K. Kruppel-like factor 4 induces p27Kip1 expression in and suppresses the growth and metastasis of human pancreatic cancer cells. Cancer Res 2008;68:4631–9. [PubMed: 18559508]

47. Wong GT, Manfra D, Poulet FM, et al. Chronic treatment with the gamma-secretase inhibitor LY-411,575 inhibits beta-amyloid peptide production and alters lymphopoiesis and intestinal cell differentiation. J Biol Chem 2004;279:12876–82. [PubMed: 14709552]

48. Searfoss GH, Jordan WH, Calligaro DO, et al. Adipsin, a biomarker of gastrointestinal toxicity mediated by a functional gamma-secretase inhibitor. J Biol Chem 2003;278:46107–16. [PubMed: 12949072]
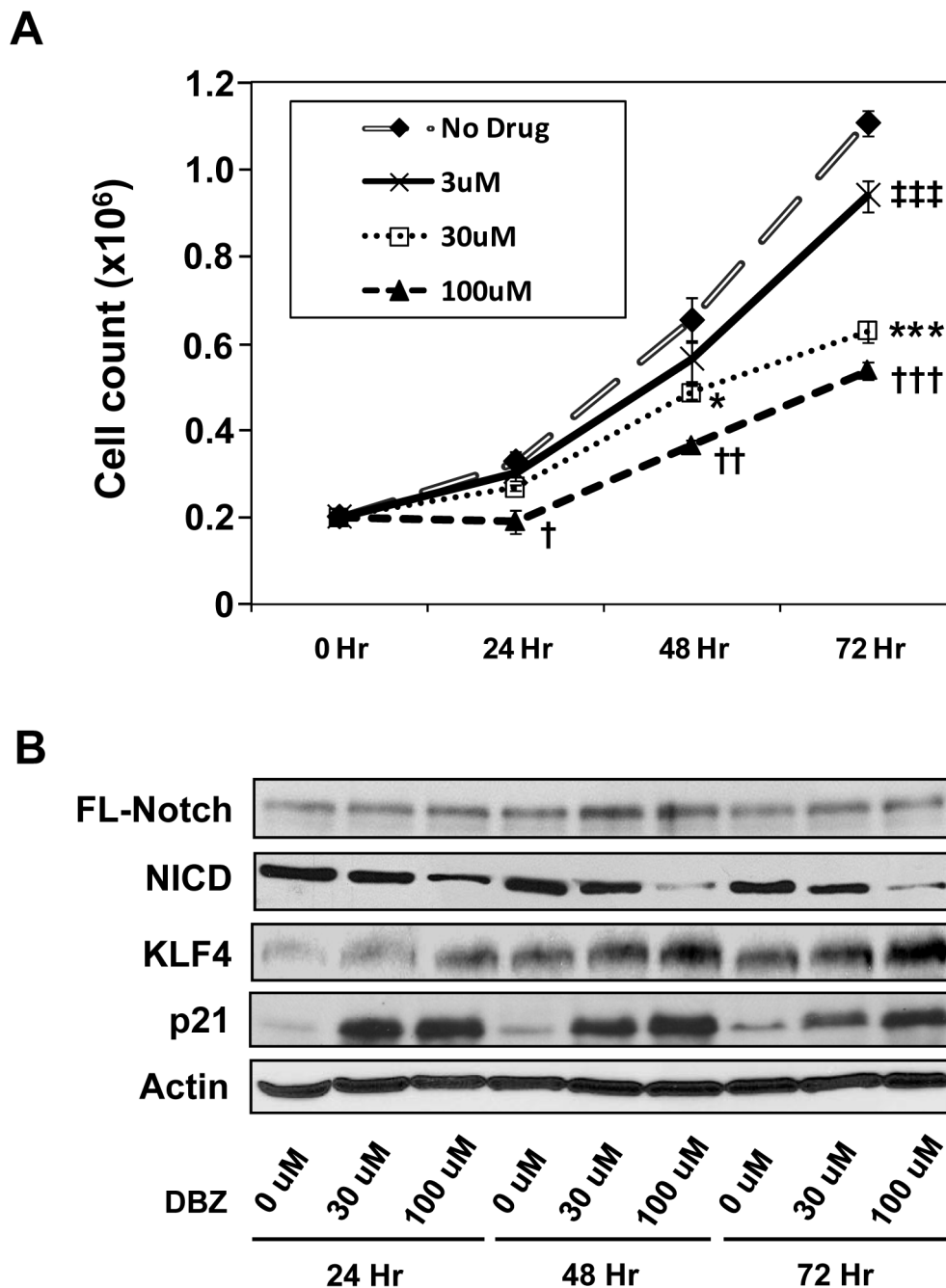
A

B

Figure 1. Suppression of Notch signaling by DBZ in HT29 cells results in decreased proliferation and increased KLF4 levels

Human colon cancer cell line HT29 was treated with increasing concentrations of the γ-secretase inhibitor, DBZ, for up to 72 hr. *(A)* Rates of proliferation were assessed by counting the number of cells daily. * and † $p < 0.05$; †† $p < 0.01$; ‡‡‡, ***, and ††† $p < 0.001$ when compared to control by paired 2-tailed *t* test. N = 4. *(B)* Western blot analysis for the indicated proteins. FL = full-length; NICD = Notch intracellular domain.
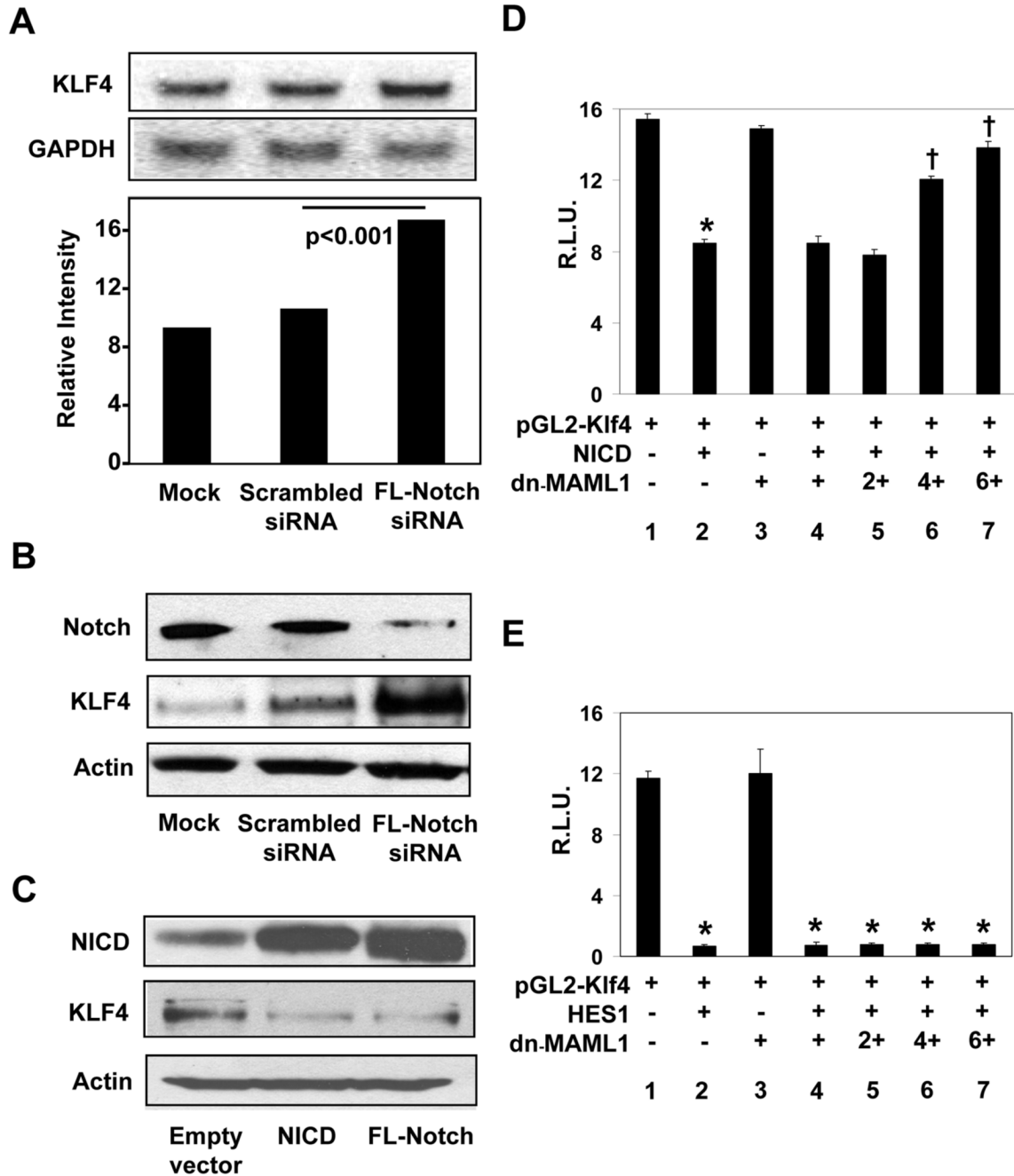
A

KLF4

GAPDH

p<0.001

Relative Intensity

Mock | Scrambled siRNA | FL-Notch siRNA

B

Notch

KLF4

Actin

Mock | Scrambled siRNA | FL-Notch siRNA

C

NICD

KLF4

Actin

Empty vector | NICD | FL-Notch

D

R.L.U.

pGL2-Klf4	+	+	+	+	+	+	+
NICD	-	+	-	+	+	+	+
dn-MAML1	-	-	+	+	2+	4+	6+
	1	2	3	4	5	6	7

E

R.L.U.

pGL2-Klf4	+	+	+	+	+	+	+
HES1	-	+	-	+	+	+	+
dn-MAML1	-	-	+	+	2+	4+	6+
	1	2	3	4	5	6	7

Figure 2. Notch suppresses KLF4 expression in HT29 cells
(*A*) HT29 cells were mock-transfected or transfected with scrambled siRNA or siRNA directed against full-length (FL) Notch. Twenty-four hr following transfection, RNA was prepared and analyzed by Northern blot analysis for KLF4 and GAPDH. The bottom graph is a densitometric tracing of KLF4 band intensities after normalizing to those of GAPDH. N = 3. (*B*) Western blot analysis of Notch, KLF4 and actin in mock-transfected HT29 cells or cells transfected with scrambled siRNA or siRNA directed against full-length Notch. (*C*) HT29 cells were transfected with empty vector, or an expression construct for NICD or full-length Notch. Western blot analysis for NICD, KLF4 and actin was performed 24 hr following transfection. (*D*) HT29 cells were co-transfected with the pGL2-Klf4 luciferase reporter (lanes 1–7), an

expression vector containing NICD (MIGR1-ICNX) (lanes 2 and 4–7), and an expression vector containing the dominant-negative MAML1 [MIGR1-MAML1 (dn-MAML1)] at increasing concentrations (lanes 3–7), along with an internal *Renilla* luciferase control. Twenty-four hr following transfection, luciferase activities were determined and normalized to the internal standard *Renilla* luciferase activities. Shown are the normalized mean relative luciferase activities (R.L.U.) from four independent experiments. * $p < 0.001$ by paired two-tailed *t* test compared to lane 1. [†] $p < 0.001$ by paired two-tailed *t* test compared to lane 2. *(E)* HT29 cells were co-transfected with the pGL2-Klf4 luciferase reporter (lanes 1–7), an expression vector containing HES1 (pCMV-HES1) (lanes 2 and 4–7), and an expression vector containing the dominant-negative MAML1 [MIGR1-MAML1 (dn-MAML1)] at increasing concentrations (lanes 3–7), along with an internal *Renilla* luciferase control. Twenty-four hr following transfection, luciferase activities were determined and normalized to the internal standard *Renilla* luciferase activities. Shown are the normalized mean relative luciferase activities (R.L.U.) from four independent experiments. *$p < 0.001$ by paired two-tailed *t* test compared to lane 1.
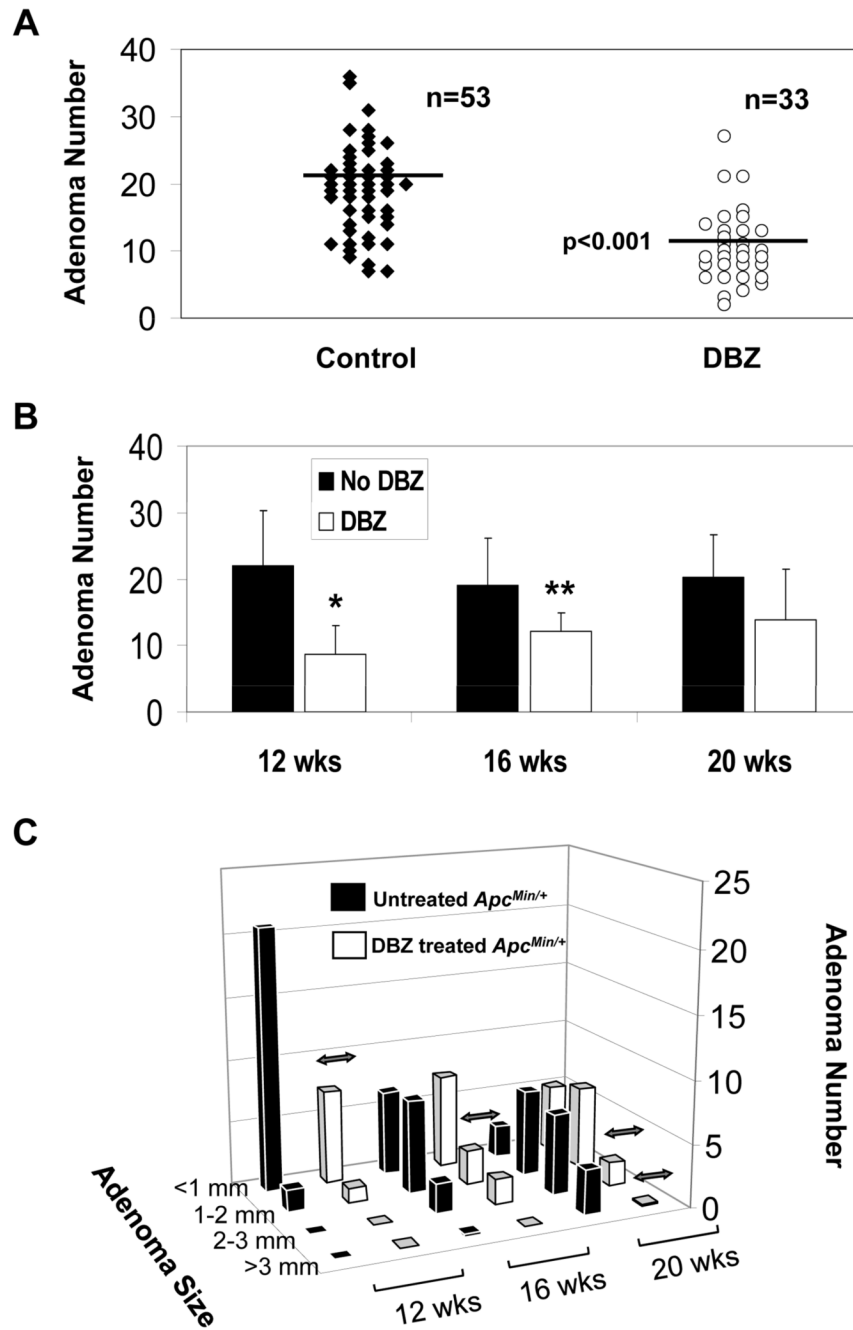
Figure 3. Effects of DBZ treatment on intestinal adenoma formation in $Apc^{Min/+}$ mice
$Apc^{Min/+}$ mice at 10, 14, or 14 weeks of age received intraperitoneal injection of vehicle or 10 μmol/kg DBZ every other day for 10 days. Two days following the last injection, mice were euthanized to determine the intestinal tumor burden. *(A)* Comparison of the number of adenomas per mouse in the small intestine between control and DBZ-treated mice in the 3 age group combined. The horizontal bars represent the mean in each group. $p < 0.001$ by paired two-tailed t test. *(B)* Comparison of the number of adenomas developed in the small intestine of control and DBZ-treated mice at 12, 16, and 20 weeks. * $p < 0.005$ and ** $p < 0.01$ by two-tailed t-test compared to control. *(C)* The size distribution of adenomas developed in the small

intestine at 12, 16 and 20 weeks, respectively, in control and DBZ-treated $Apc^{Min/+}$ mice. Double-headed arrows indicate significant difference between the two groups ($p < 0.01$).
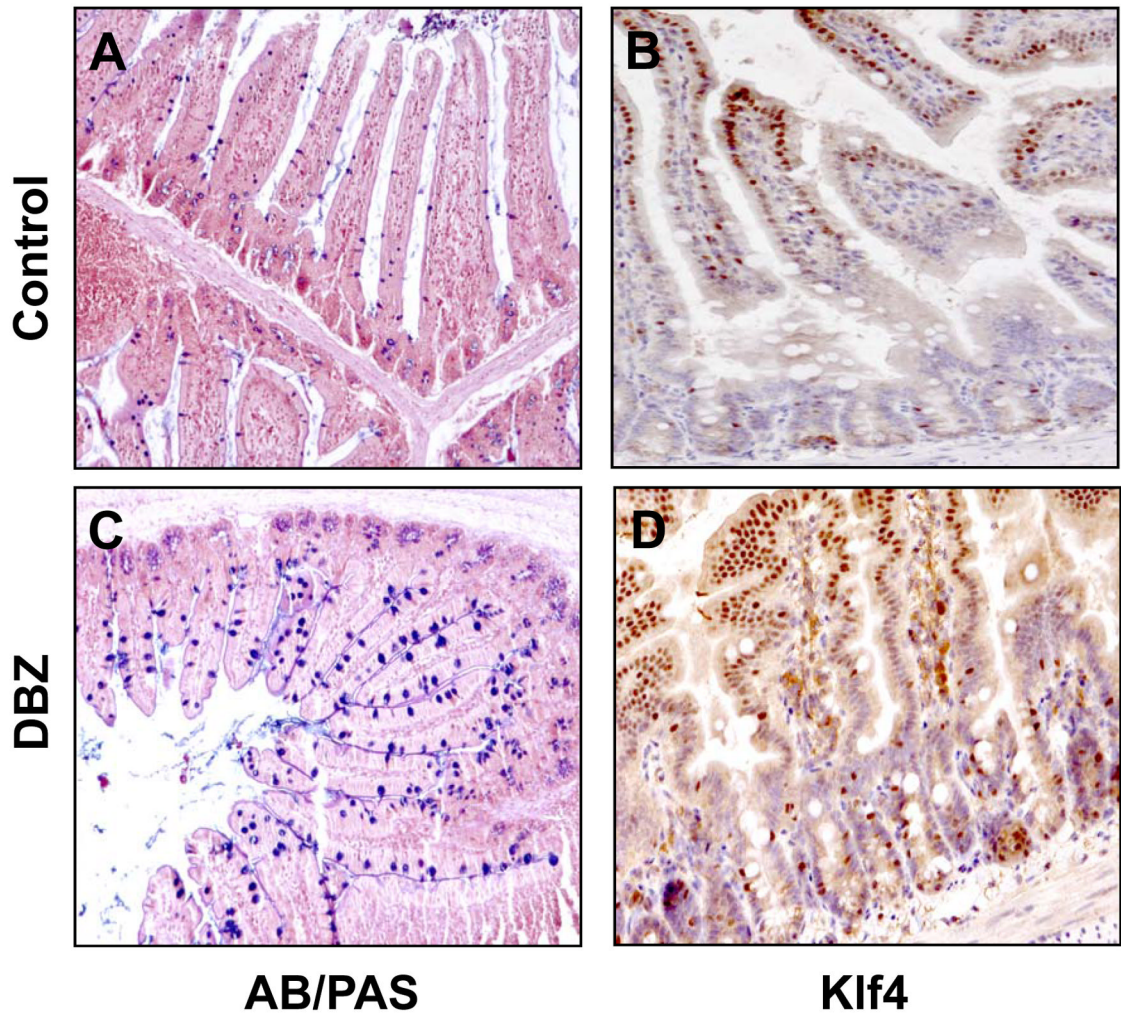
$Apc^{Min/+}$ (Normal Mucosa)

Figure 4. Histochemical staining for goblet cells and immunostaining for Klf4 in the normal-appearing small intestinal mucosa of control and DBZ-treated $Apc^{Min/+}$ mice
The normal-appearing small intestinal tissues obtained from age-matched control (*A* and *B*) and DBZ-treated (*C* and *D*) $Apc^{Min/+}$ mice were stained for goblet cells (blue) using alcian blue/periodic acid-Schiff (AB/PAS) stain (*A* and *C*) or immunostained for Klf4 (*B* and *D*).
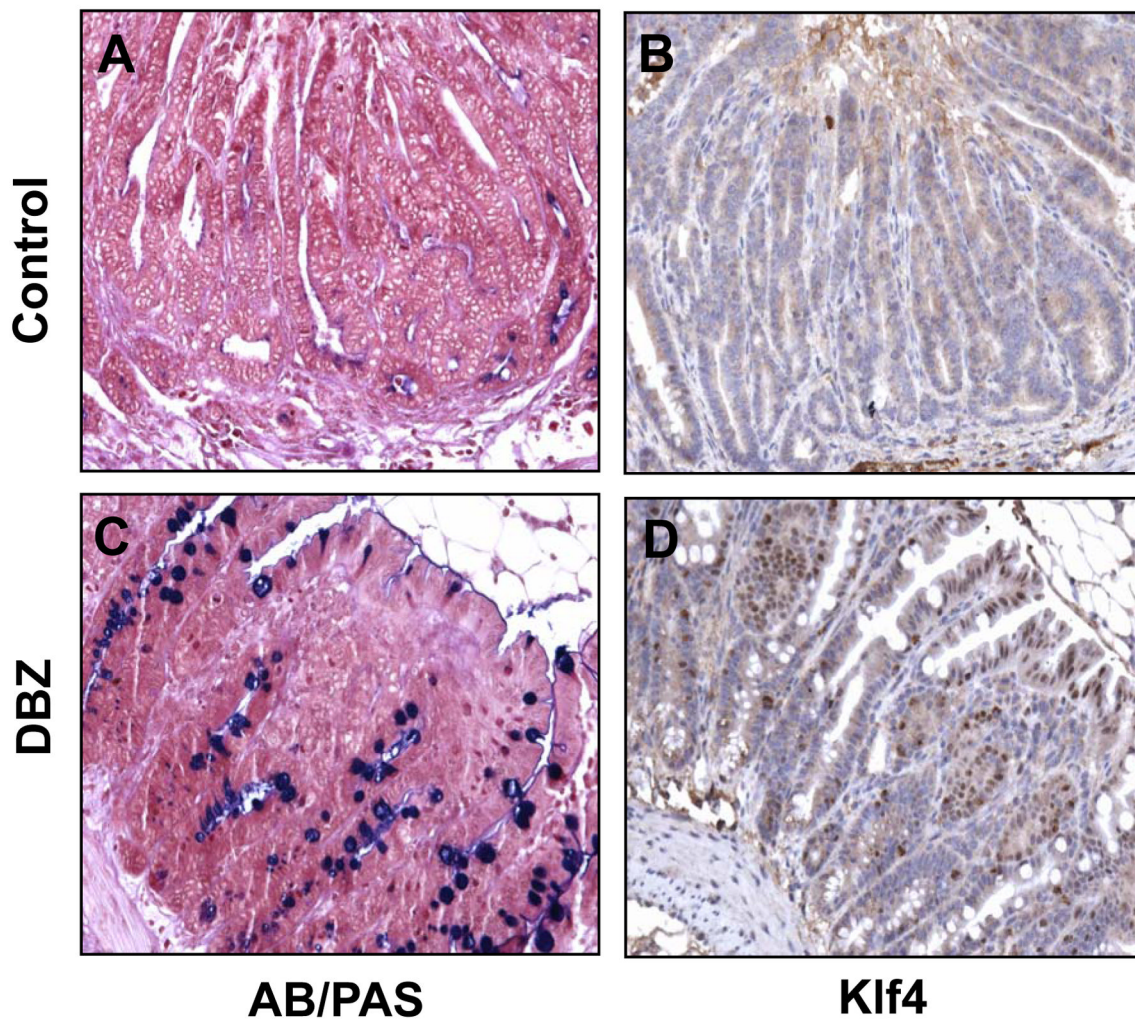
Apc^{Min/+} (Adenoma)

Figure 5. AB/PAS staining and Klf4 immunostaining in intestinal adenomas from control and DBZ-treated *Apc^{Min/+}* mice
Small intestinal adenomas obtained from age-matched control (*A* and *B*) and DBZ-treated
(*C* and *D*) *Apc^{Min/+}* mice were stained for goblet cells (blue) using alcian blue/periodic acid-
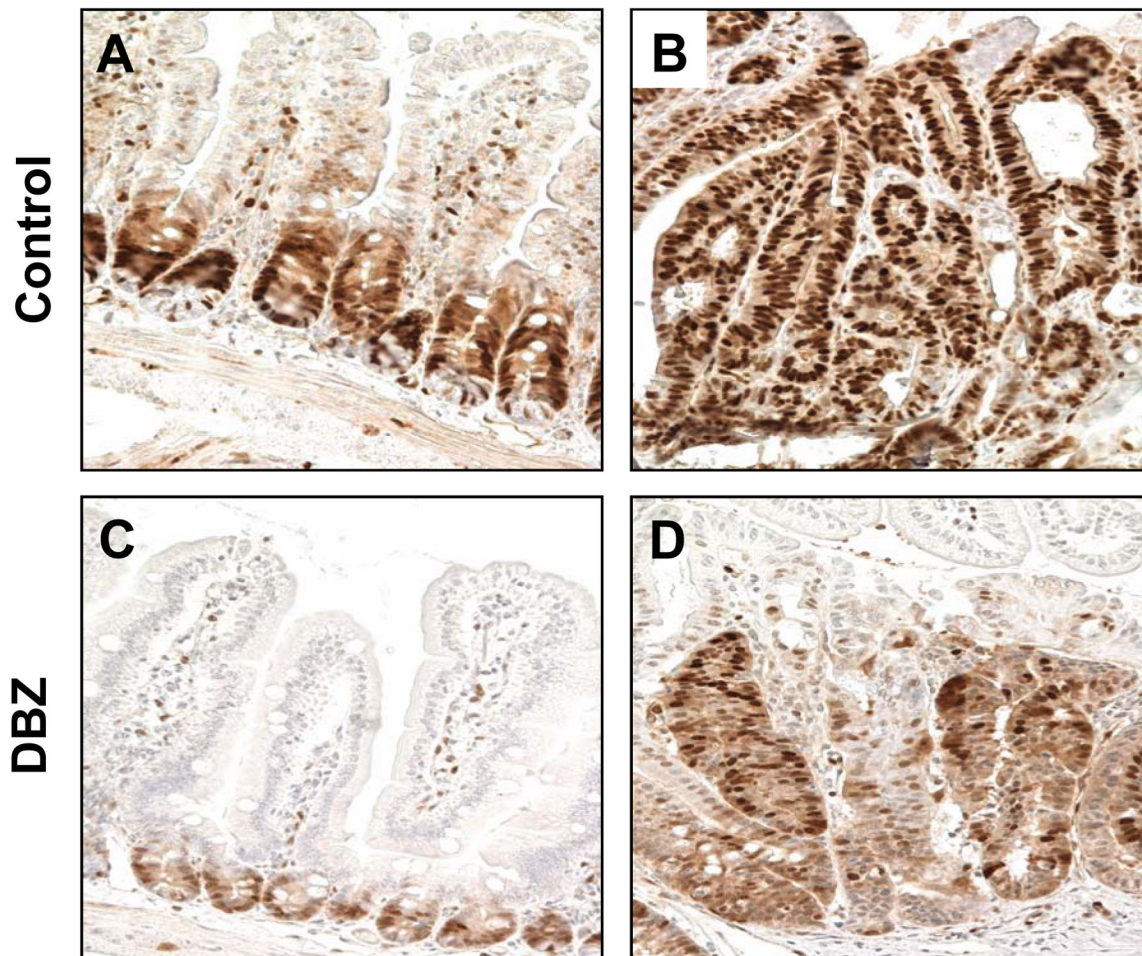Schiff (AB/PAS) stain (*A* and *C*) or immunostained for Klf4 (*B* and *D*).

Apc^{*Min/+*} (Cyclin D1)

Figure 6. Cyclin D1 immunostaining in the normal-appearing small intestinal mucosa and adenomas from control and DBZ-treated *Apc*$^{Min/+}$ mice
Normal-appearing small intestinal tissues (***A*** and ***C***) and small intestinal adenomas (***B*** and ***D***) obtained from age-matched control *Apc*$^{Min/+}$ mice (***A*** and ***B***) and DBZ-treated *Apc*$^{Min/+}$ mice (***C*** and ***D***) were immunostained with antibodies against cyclin D1.